Published in final edited form as:
Eur Radiol. 2012 July ; 22(7): 1592–1600. doi:10.1007/s00330-012-2404-7.

Comparison of clinical semi-quantitative assessment of muscle fat infiltration with quantitative assessment using chemical shift-based water/fat separation in MR studies of the calf of post-menopausal women

Hamza Alizai, **Lorenzo Nardo**, **Dimitrios C. Karampinos**, **Gabby B. Joseph**, **Samuel P. Yap**, **Thomas Baum**, **Roland Krug**, **Sharmila Majumdar**, and **Thomas M. Link**
Musculoskeletal and Quantitative Imaging Research Group, Department of Radiology and Biomedical Imaging, University of California, San Francisco, 185 Berry Street, Suite 350, San Francisco, CA 94107, USA

Hamza Alizai: Hamza.Alizai@ucsf.edu

Abstract

Objective—The goal of this study was to compare the semi-quantitative Goutallier classification for fat infiltration with quantitative fat-fraction derived from a magnetic resonance imaging (MRI) chemical shift-based water/fat separation technique.

Methods—Sixty-two women (age 61±6 years), 27 of whom had diabetes, underwent MRI of the calf using a T1-weighted fast spin-echo sequence and a six-echo spoiled gradient-echo sequence at 3 T. Water/fat images and fat fraction maps were reconstructed using the IDEAL algorithm with T2* correction and a multi-peak model for the fat spectrum. Two radiologists scored fat infiltration on the T1-weighted images using the Goutallier classification in six muscle compartments. Spearman correlations between the Goutallier grades and the fat fraction were calculated; in addition, intra-observer and inter-observer agreement were calculated.

Results—A significant correlation between the clinical grading and the fat fraction values was found for all muscle compartments (P<0.0001, R values ranging from 0.79 to 0.88). Goutallier grades 0–4 had a fat fraction ranging from 3.5 to 19%. Intra-observer and inter-observer agreement values of 0.83 and 0.81 were calculated for the semi-quantitative grading.

Conclusion—Semi-quantitative grading of intramuscular fat and quantitative fat fraction were significantly correlated and both techniques had excellent reproducibility. However, the clinical grading was found to overestimate muscle fat.

Keywords

Skeletal muscle; Magnetic resonance imaging; Adipose tissue; Metabolic syndrome; Neuromuscular disease; Sarcopenia

Introduction

Fatty infiltration of muscle has been observed in numerous chronic conditions. These include metabolic disorders such as obesity and diabetes, sarcopaenia due to ageing, neurogenic disorders such as chronic denervation and muscular dystrophies, iatrogenic

Correspondence to: Hamza Alizai, Hamza.Alizai@ucsf.edu.

effects of glucocorticoid use and as a late outcome of severe muscle and tendon injuries [1–3]. Non-invasive semi-quantitative imaging-based evaluation of the fatty infiltration of muscle is an important diagnostic measurement and can be a determinant of the most appropriate management for the patient.

Type 2 diabetes mellitus (T2DM) is a chronic disease of metabolism and individuals with T2DM-related peripheral neuropathy develop muscle weakness, motor dysfunction and loss of strength; especially in the distal lower extremity [4–6]. Intermuscular adipose tissue (IMAT) [7], defined as the adipose tissue visible on T1-weighted images beneath the muscle fascia and between muscle groups along with intramuscular adipose tissue distributed within the muscle, is increased in T2DM and negatively associated with insulin sensitivity [8, 9]. Furthermore, IMAT and intramuscular adipose tissue have a strong negative correlation with physical performance in the calf muscle of individuals with metabolic syndrome including T2DM and obesity [3, 9].

Computed tomography (CT) and magnetic resonance imaging (MRI) have both been used to assess the degree of fat infiltration of muscle [10–13]. The established clinical semi-quantitative scales for intramuscular fat are based on the visual assessment of the amount of fatty infiltration of the muscle on T1-weighted images, which ranges from normal appearance to complete fatty infiltration [13–17]. The most commonly used grading in the clinical setting is the Goutallier classification of fatty muscle degeneration [13].

MRI can also be used to quantitatively assess fat content and chemical shift-based water/fat separation is an alternative technique for evaluation of the fat fraction based on the different precession frequencies of water and lipid hydrogen protons [18–20]. The technique can provide an accurate measure of the at fraction and is currently an emerging clinical application. Quantitative MRI techniques assessing the skeletal muscle fat fraction have been validated and determined to provide an accurate, reliable calculation of the muscle fat fraction, which is consistent with muscle biopsies [10].

MRI chemical shift-based water/fat-saturation techniques require, however, the implementation of advanced image processing algorithms that may not be available in a clinical setting. A fast, reproducible and easy to use semi-quantitative scale for fat infiltration would therefore be crucial in implementing measurements of fat infiltration clinically. However, to the best of our knowledge, there are no studies that determine the accuracy of visual classification systems such as Goutallier. As invasive histological studies are not feasible for validating a semiquantitative score in a clinical setting, comparison with validated quantitative MR techniques provides an alternative for assessing the accuracy of semi-quantitative classifications for fat infiltration. The goal of this study was therefore to assess the reproducibility of the semi-quantitative Goutallier classification for fat infiltration of the calf muscle and validate this grading system with the quantitative muscle fat fraction derived from a MRI chemical shift-based water/fat separation technique.

Materials and methods

Subjects

Post–menopausal women with an age range of 50–75 years and a body mass index (BMI) of 21–35 kg/m^2 with and without a history of T2DM were recruited for the study. A total of 62 women (with a mean age 62.3±5.8 years) participated in the study (35 women without diabetes and 27 women with diabetes). The 35 healthy subjects without T2DM had a mean age of 61.9±6.1 years and BMI of 25.8±4.2 kg/m^2. The 27 subjects with T2DM had a mean age of 62.7±5.4 years and BMI of 27.5±3.6 kg/m^2; differences were non-significant (P>0.05).

The study was approved by the local Institutional Review Board and conducted in accordance with the Committee for Human Research (CHR) at the University of California, San Francisco. All subjects received and signed written informed consent before participation in the study.

MRI

The 62 post-menopausal subjects underwent MRI of the right middle-calf muscle region with a 3.0-Tesla whole-body MR system (Signa HDx; GE Healthcare, Waukesha, WI, USA) using an eight-channel lower extremity transmit–receive coil. Axial T1-weighted images were acquired using a fast spin-echo (FSE) sequence with the following parameters: TR/TE=600/9 ms, ETL=7, receiver bandwidth= 31.25 kHz, NEX=2, 384×192 acquisition matrix size, FOV=18 cm, 60 slices with 2-mm thickness. The axial T1-weighted sequences served to semi-quantitatively assess fat infiltration. Axial T2-weighted images were also acquired using a fast spin-echo sequence with the following parameters: TR/TE =6,000/47 ms, ETL =12, receiver bandwidth=31.25 kHz, NEX=2, 384×192 acquisition matrix size, FOV=18 cm, 60 slices with 2-mm thickness.

For chemical shift-based fat quantification, a two-shot, six-echo, three-dimensional (3D) spoiled gradient-echo sequence (SPGR) with monopolar readout gradients was used to acquire multi-echo images (six echoes). This sequence had the following parameters: TR/TE/ΔTE=12/1.4/0.7 ms, flip angle=3°, receiver bandwidth=83.33 kHz, 180×180 acquisition matrix size, FOV=18 cm, 30 slices with 4-mm thickness.

Water and fat images were reconstructed online using an investigational version of the chemical shift-based water–fat separation method known as the iterative decomposition of water and fat with echo asymmetry and least-squares estimation (IDEAL) [20]. A region-growing algorithm was employed for the field-map estimation to avoid water/fat swaps as in [21]. The employed water/fat signal separation approach used a single T2* correction [22] and the pre-calibrated multi-peak fat spectrum [23] to account for the presence of multiple peaks in the fat spectrum [24]. A flip angle of 3° was used to minimise the T1-induced bias on fat fraction estimates [25–27]. Additional considerations of the employed water/fat separation approach included the implementation of a hybrid approach combining magnitude and complex fitting to compensate for eddy current effects [28] and the implementation of the magnitude discrimination approach to remove noise-induced bias at low and high fat fractions [27]. Based on the water/fat separated images, in-phase images were formed by computing the sum of the separated water and fat images and out-of-phase images were formed by computing the absolute value to the difference of the separated water and fat images. Finally, fat fraction maps were formed by computing the ratio of the separated fat signal over the sum of the separated water and fat signals.

Image analysis: quantitative assessment

Post-processing was performed using in-house-built routines in MATLAB (The Mathworks, Natick, MA, USA). The segmentation of all muscle compartments was performed manually by a trained radiologist. The T2-weighted images were segmented to define six muscular regions: three muscles (medial gastrocnemius [MG], lateral gastrocnemius [LG], soleus [SOL]) and three muscle compartments (anterior compartment [AC]: tibialis anterior, extensor digitorum, extensor hallucis; deep posterior compartment [DP]: tibialis posterior, flexor digitorum, flexor hallucis; and the lateral compartment [LC]: peroneus longus and brevis). Figure 1 demonstrates a T2-weighted image of the calf with manual segmentation of the six muscle compartments: AC, SOL, DP, MG, LG and LC. The manual drawing of the regions of interest (ROIs) for the six muscle compartments was performed so that the boundaries of the ROIs were within 2–3 mm from the muscle boundaries and the muscle

fascia, as visually inspected on the T2-weighted images. Mean fat fraction values were then generated by taking the mean of the IDEAL-derived fat fraction over the manually drawn ROIs. Mean fat fraction was generated using predetermined slices in proximal, middle and distal regions of the scanned calf region to assess anatomical variations in the fat infiltration.

Image analysis: semi-quantitative assessment

Two radiologists analysed T1-weighted images for all 62 patients and graded the presence of fatty infiltration based on a five-point semi-quantitative scale described by Goutallier et al. [13]: grade 0, normal; grade 1, some fatty streaks; grade 2, less fat than muscle; grade 3; fatty degeneration of 50%; grade 4, fatty infiltration of more than 50%; Fig. 2 illustrates T1-weighted images of the calf with Goutallier grades 1–4. In the event of disagreement during clinical grading, a consensus reading with a third musculoskeletal radiologist with 24 years' experience in musculoskeletal imaging was performed. Each subject's calf muscle fat infiltration was graded in the six muscle compartments (AC, SOL, MG, LG, DP and PER) and the three anatomical locations (proximal, middle and distal calf) where the chemical shift-based mean fat fraction was calculated. The radiologists were blinded to the patient identifiers, demographics and the calculated fat fraction values.

Statistical analysis

Statistical analysis was performed using STATA 11 software (StataCorp, College Station, TX, USA). Descriptive statistics (i.e. mean age, BMI, etc.) were calculated for all patients. The correlation between muscle fat fraction versus semi-quantitative grade was assessed using Spearman's correlations with Bonferroni corrections. A regression model was used to assess the difference between the mean fat fraction and the clinical grades. A regression model was also used to analyse the difference in the mean fat fraction among the proximal, middle and distal regions of the calf. A chi-squared test was performed to assess the difference in clinical grades between the subjects with diabetes and the subjects without diabetes.

Reproducibility analysis

The manual segmentation of the calf muscle compartments was repeated three times in five randomly selected subjects by one radiologist to assess the intra-observer reproducibility of the segmentation process. Coefficients of variation (CVs) for the volume of intramuscular fat were calculated.

Two radiologists independently graded 12 randomly selected studies according to Goutallier classification two times. After an interval of 1 month, the grading of these studies was repeated to determine intra-observer reliability. Cohen's Kappa values were calculated to assess intra-observer and inter-observer reliability of the muscle fat infiltration grade based on the Goutallier classification [29].

Results

Distribution of Goutallier grades

Figure 3 illustrates the frequency of clinical grades 0–4 for the six muscle compartments. As expected for a population of relatively healthy individuals, low Goutallier grades of 0 and 1 had the highest frequency. Grading muscle fat in six muscle compartments in the three regions of the calf resulted in a total of 1,039 clinical grades after exclusion of images at the edges of the examined 3D volume (i.e. images suffering from slab profile effects). When analysing the distribution of clinical grades in all muscle compartments and all three regions of the calf, grade 1 was the most common, consisting of 56.07% of the overall grading, followed by grades 0, 2, 3 and 4, which consisted of 20.81, 17.92, 0.04 and 0.02% of the

total grades, respectively. Lower Goutallier grades (0 and 1) were most common in AC, where they consisted of 89% of overall grading, while the higher clinical grades of 3 and 4 were most common in PER and MG, where they comprised 9% and 6% respectively of the overall grades.

Lower grades were more common in the subjects who were not diabetic; 26% were grade 0 and 56% were grade 1, while 14% of the total grades were grade 0 and 56% were grade 1 for diabetic subjects. There was a reverse trend seen for the higher clinical grades; grades 2, 3 and 4 consisted of 15%, 2% and 1% of total grades in subjects without diabetes, while they comprised 21%, 6% and 3% of total grades in patients with diabetes. No significant difference was found between the Goutallier grades in the diabetic and the non-diabetic groups.

Association between Goutallier grade and fat fraction

Tables 1, 2 and 3 list the mean fat fraction subdivided by Goutallier grade and muscle compartment in the proximal (Table 1), middle (Table 2) and distal (Table 3) regions of the calf. The mean fat fraction values consistently increased with increasing Goutallier grade. There was a significant difference in the mean fat fraction among the five clinical grades in each muscle compartment and in all three regions ($P<0.01$). There was no significant difference in the mean fat fraction of the proximal, middle and distal regions, when assessed by selecting individual muscle compartments and by each clinical grade. When averaging the fat fraction in the six muscle compartments, there was still no difference found in mean fat fraction among the three regions of the calf.

Figure 4 demonstrates the varying mean fat fractions in the six muscle compartments (AC, SOL, MG, LG, PER and DP) in comparison with the clinical grades. The mean fat fractions calculated were lower than the muscle fat description of the corresponding clinical grades. A clinical grade of 1, which is defined as some fatty streaks, represented an average mean fat fraction of only 6.5%±1.4%; grade 2 defined as less fat than muscle, had a mean fat fraction of 9.8%±1.7%; grade 3 described as the same amount of fat as muscle had an average fat fraction of 14.3%±0.9%; and grade 4, which is defined as more fat than muscle, had an average fat fraction of only 19%±4.4%. A clinical grade of 0, which is defined as a normal appearance of muscle with an absence of fat had an average mean fat fraction of 3.5%± 0.6%.

A Goutallier grade of 2 is considered the transition point from normal to pathological fatty infiltration [13, 30], with a higher grade than 2 even being considered as a negative prognostic factor for muscle recovery. We therefore used grade 2 as the reference in the regression model and compared the fat fraction in the remaining grades with that of grade 2. The mean fat fraction in grade 2 was significantly lower than that in grade 3 in all muscle compartments and in all regions of the calf ($P<0.01$).

A significant correlation between the semi-quantitative clinical grading and the fat fraction calculated using the chemical shift based water/fat separation technique was found for all muscle compartments ($P<0.0001$). Table 4 lists the Spearman's correlations between the quantitatively derived mean fat fraction and the semi-quantitative clinical grading, with Bonferroni correction in the proximal, middle and distal regions of the calf (all P values <0.0001). Average R values of 0.85, 0.82, 0.83, 0.86, 0.88 and 0.79 were calculated for the correlation between the two analyses in AC, DP, LG, MG, PER and SOL respectively. Average R values of 0.832, 0.808 and 0.872 were calculated for the correlation among Goutallier grades and the mean fat fraction in the proximal, middle and distal calf respectively.

Reproducibility analysis

The coefficient of variation for intra-observer reproducibility of intramuscular fat based on masks generated by manual segmentation of the six calf muscle compartments was 2.7%. Cohen's Kappa values calculated for intra-observer and inter-observer agreement of the semi-quantitative clinical grading of T1-weighted images based on Goutallier classification were 0.83 and 0.81 respectively, which is classified as substantial to near perfect agreement.

Discussion

Our study shows that there is a significant correlation between the mean fat fraction calculated using MR chemical shift-based water/fat separation and the clinical semi-quantitative scoring system for fatty infiltration described by Goutallier et al. [13]. However, the mean fat fractions calculated were much lower than the muscle fat description of the corresponding clinical Goutallier grades. The range of mean fat fraction described in the literature is highly variable; 8% in normal controls to 48% using the two-point Dixon technique [18, 31] in patients with oculopharyngeal muscular dystrophy, from 0.7 to 12% in a cohort of healthy subjects with relatives diagnosed with T2DM using a fat-selective spectral–spatial sequence [32]; our results showed a range of 3–19%. A possible explanation for the observed overestimation of fat content using the clinical grading is the spatially heterogeneous fat infiltration in the patients; the clinical grading based on the visual assessment of the T1-weighted images cannot differentiate a voxel with an intermediate fat fraction from a voxel with a high fat fraction. Additionally, the inclusion of connective tissue, small neural and vascular structures in the visual assessment of fat may further contribute to the overestimation of fat content.

Clinical semi-quantitative grades present a fast reproducible mode of quantifying muscle but lack sensitivity to subtle changes in muscle fat. The Goutallier classification was originally described for the purposes of assessing fatty infiltration on CT images [13]. Fuchs et al. [17] used this classification for the assessment of muscle fat on MRI with Goutallier's classification on CT as a reference; they found MRI to have a better inter-observer reliability than CT. This scoring system has been widely accepted in the orthopaedic literature and used extensively for determining management of rotator cuff tears [2]. Other MRI-based visual scoring systems for dystrophic changes of muscle and fatty infiltration in inherited neuromuscular disorders have been described by Fischer et al. [16], Kornblum et al. [15] and Mercuri et al. [14]. However, a correlation among these radiological classifications and the macroanatomical or histological presence of fat in the graded muscles is not established [17].

To the best of our knowledge, fat quantification has not been extensively studied in normal skeletal muscle. The calf muscle was used in this study because of its clinical importance in the pathophysiology of metabolic syndrome, which includes T2DM and inherited neuromuscular disorders such as Limb–Girdle muscular dystrophies [33]. T2DM and peripheral neuropathy are associated with an increase in IMAT in the leg, which has been suggested as a possible explanation for the low calf muscle power and impaired physical function in these patients [3].

Metabolic syndrome has a high reported prevalence of 24% in the US population [34] and its known complication includes neuromuscular problems of the distal limbs [31]. The applications of quantitative MR techniques in metabolic syndrome have been the subject of recent studies with a focus on the content, localisation and composition of fat within the skeletal muscle as determinants of insulin resistance [3, 11, 35, 36]. Gallagher et al. [36] found that subjects with T2DM had a greater amount of IMAT than healthy controls. The increase in muscle fat affects insulin sensitivity, glucose and lipid metabolism, which can

identify the phenotype of a normal-weight, metabolically obese individual [35]; quantitative imaging can play a role in an early diagnosis and intervention in this population. Life-style interventions such aerobic exercise reduce IMAT, which has been found to correlate with serum lipid levels and can result in some improvement in dyslipidaemia [37]. Sensitive quantitative MR techniques such as the one utilised in the present study can play an important role in enhancing our knowledge of muscle fat and its association with pathological conditions including T2DM.

The study had some limitations. First, an average of 2 hours were required to segment each calf; a limitation of the present approach that can be eliminated by using semi-automatic segmentation software. The manual segmentation technique used in the study, however, was found to have good reproducibility.

Another limitation of the study was the low frequency of higher clinical grades including grades 3 and 4, which is to be expected in a relatively healthy subject population. The higher frequency of clinical grade 1 rather than grade 0 in this study can be explained by the subjects being older post-menopausal women, some of them diabetic; muscular fat is known to be associated with ageing and metabolic disorders such as obesity and diabetes [7, 35].

To conclude, clinical grading of fat infiltration using the Goutallier classification and fat fraction values derived using chemical shift-based water/fat separation techniques (IDEAL) were significantly correlated and high intra-observer and inter-observer agreement values were found. However, the clinical grading based on the Goutallier classification was found to overestimate muscle fat. While clinical grading provides a fast, reproducible method of analysing muscle fat, a quantitative technique like IDEAL provides more accurate information about the muscle fat content and will be invaluable for monitoring the disease process, subtle progression and efficacy of treatment. Further studies need to be performed, however, before these sophisticated techniques can be implemented in a clinical setting.

Acknowledgments

This study was supported by the National Institutes of Health grants R01-AG17762 and RC1-AR058405.

References

1. Wren TA, Bluml S, Tseng-Ong L, Gilsanz V. Three-point technique of fat quantification of muscle tissue as a marker of disease progression in Duchenne muscular dystrophy: preliminary study. AJR Am J Roentgenol. 2008; 190:W8–W12. [PubMed: 18094282]
2. Cheung S, Dillon E, Tham SC, et al. The presence of fatty infiltration in the infraspinatus: its relation with the condition of the supraspinatus tendon. Arthroscopy. 2011; 27:463–470. [PubMed: 21277734]
3. Hilton TN, Tuttle LJ, Bohnert KL, Mueller MJ, Sinacore DR. Excessive adipose tissue infiltration in skeletal muscle in individuals with obesity, diabetes mellitus, and peripheral neuropathy: association with performance and function. Phys Ther. 2008; 88:1336–1344. [PubMed: 18801853]
4. Andersen H, Gadeberg PC, Brock B, Jakobsen J. Muscular atrophy in diabetic neuropathy: a stereological magnetic resonance imaging study. Diabetologia. 1997; 40:1062–1069. [PubMed: 9300243]
5. Andersen H, Nielsen S, Mogensen CE, Jakobsen J. Muscle strength in type 2 diabetes. Diabetes. 2004; 53:1543–1548. [PubMed: 15161759]
6. Andersen H, Poulsen PL, Mogensen CE, Jakobsen J. Iso-kinetic muscle strength in long-term IDDM patients in relation to diabetic complications. Diabetes. 1996; 45:440–445. [PubMed: 8603765]
7. Gallagher D, Kuznia P, Heshka S, et al. Adipose tissue in muscle: a novel depot similar in size to visceral adipose tissue. Am J Clin Nutr. 2005; 81:903–910. [PubMed: 15817870]

8. Goodpaster BH, Thaete FL, Kelley DE. Thigh adipose tissue distribution is associated with insulin resistance in obesity and in type 2 diabetes mellitus. Am J Clin Nutr. 2000; 71:885–892. [PubMed: 10731493]
9. Frimel TN, Sinacore D, Wright NR, Villareal DT, Klein S. Sarcopenia in frail elderly obese participants: role of excess skeletal muscle lipid accumulation. J Geriatr Phys Ther. 2007; 30:138.
10. Gaeta M, Scribano E, Mileto A, et al. Muscle fat fraction in neuromuscular disorders: dual-echo dual-flip-angle spoiled gradient-recalled MR imaging technique for quantification—a feasibility study. Radiology. 201110.1148/radiol.10101108
11. Karampinos DC, Baum T, Nardo L, et al. Characterization of regional distribution of skeletal muscle adipose tissue in type 2 diabetes using chemical shift-based water/fat separation. J Magn Reson Imaging. 201110.1002/jmri.23512
12. Pfirrmann CWA, Schmid MR, Zanetti M, Jost B, Gerber C, Hodler J. assessment of fat content in supraspinatus muscle with proton MR spectroscopy in asymptomatic volunteers and patients with supraspinatus tendon lesions1. Radiology. 2004; 232:709–715. [PubMed: 15333791]
13. Goutallier D, Postel J-M, Bernageau J, Lavau L, Voisin M-C. Fatty muscle degeneration in cuff ruptures: pre- and postoperative evaluation by CT scan. Clin Orthop Relat Res. 1994; 304:78–83. [PubMed: 8020238]
14. Mercuri E, Talim B, Moghadaszadeh B, et al. Clinical and imaging findings in six cases of congenital muscular dystrophy with rigid spine syndrome linked to chromosome 1p (RSMD1). Neuromuscul Disord. 2002; 12:631–638. [PubMed: 12207930]
15. Kornblum C, Lutterbey G, Bogdanow M, et al. Distinct neuromuscular phenotypes in myotonic dystrophy types 1 and 2: a whole body highfield MRI study. J Neurol. 2006; 253:753–761. [PubMed: 16511650]
16. Fischer D, Kley RA, Strach K, et al. Distinct muscle imaging patterns in myofibrillar myopathies. Neurology. 2008; 71:758–765. [PubMed: 18765652]
17. Fuchs B, Weishaupt D, Zanetti M, Hodler J, Gerber C. Fatty degeneration of the muscles of the rotator cuff: assessment by computed tomography versus magnetic resonance imaging. J Shoulder Elbow Surg. 1999; 8:599–605. [PubMed: 10633896]
18. Dixon WT. Simple proton spectroscopic imaging. Radiology. 1984; 153:189–194. [PubMed: 6089263]
19. Glover GH, Schneider E. Three-point Dixon technique for true water/fat decomposition with B0 inhomogeneity correction. Magn Reson Med. 1991; 18:371–383. [PubMed: 2046518]
20. Reeder SB, Pineda AR, Wen Z, et al. Iterative decomposition of water and fat with echo asymmetry and least-squares estimation (IDEAL): application with fast spin-echo imaging. Magn Reson Med. 2005; 54:636–644. [PubMed: 16092103]
21. Yu H, Reeder SB, Shimakawa A, Brittain JH, Pelc NJ. Field map estimation with a region growing scheme for iterative 3-point water-fat decomposition. Magn Reson Med. 2005; 54:1032–1039. [PubMed: 16142718]
22. Yu H, McKenzie CA, Shimakawa A, et al. Multiecho reconstruction for simultaneous water-fat decomposition and T_2* estimation. J Magn Reson Imaging. 2007; 26:1153–1161. [PubMed: 17896369]
23. Middleton, MS.; Hamilton, G.; Bydder, M.; Sirlin, CB. How much fat is under the water peak in liver fat MR spectroscopy?. Proceedings of the 17th Annual Meeting of ISMRM; Honolulu. 2009. p. 4331
24. Yu H, Shimakawa A, McKenzie CA, Brodsky E, Brittain JH, Reeder SB. Multiecho water-fat separation and simultaneous R_2* estimation with multifrequency fat spectrum modeling. Magn Reson Med. 2008; 60:1122–1134. [PubMed: 18956464]
25. Karampinos DC, Yu H, Shimakawa A, Link TM, Majumdar S. T(1)-corrected fat quantification using chemical shift-based water/fat separation: application to skeletal muscle. Magn Reson Med. 2011; 66:1312–1326. [PubMed: 21452279]
26. Bydder M, Yokoo T, Hamilton G, et al. Relaxation effects in the quantification of fat using gradient echo imaging. Magn Reson Imaging. 2008; 26:347–359. [PubMed: 18093781]

27. Liu CY, McKenzie CA, Yu H, Brittain JH, Reeder SB. Fat quantification with IDEAL gradient echo imaging: correction of bias from T_1 and noise. Magn Reson Med. 2007; 58:354–364. [PubMed: 17654578]
28. Yu H, Shimakawa A, Hines CD, et al. Combination of complex-based and magnitude-based multiecho water-fat separation for accurate quantification of fat-fraction. Magn Reson Med. 2011; 66:199–206. [PubMed: 21695724]
29. Landis JR, Koch GG. The measurement of observer agreement for categorical data. Biometrics. 1977; 33:159–174. [PubMed: 843571]
30. Goutallier D, Postel JM, Lavau L, Bernageau J. Impact of fatty degeneration of the suparspinatus and infraspinatus msucles on the prognosis of surgical repair of the rotator cuff. Rev Chir Orthop Reparatrice Appar Mot. 1999; 85:668–676. [PubMed: 10612130]
31. Gloor M, Fasler S, Fischmann A, et al. Quantification of fat infiltration in oculopharyngeal muscular dystrophy: comparison of three MR imaging methods. J Magn Reson Imaging. 2011; 33:203–210. [PubMed: 21182140]
32. Machann J, Bachmann OP, Brechtel K, et al. Lipid content in the musculature of the lower leg assessed by fat selective MRI: intra- and interindividual differences and correlation with anthropometric and metabolic data. J Magn Reson Imaging. 2003; 17:350–357. [PubMed: 12594726]
33. Wattjes M, Kley R, Fischer D. Neuromuscular imaging in inherited muscle diseases. Eur Radiol. 2010; 20:2447–2460. [PubMed: 20422195]
34. Ford ES, Giles WH, Dietz WH. Prevalence of the metabolic syndrome among US adults: findings from the third National Health and Nutrition Examination Survey. JAMA. 2002; 287:356–359. [PubMed: 11790215]
35. Vettor R, Milan G, Franzin C, et al. The origin of intermuscular adipose tissue and its pathophysiological implications. Am J Physiol Endocrinol Metab. 2009; 297:E987–E998. [PubMed: 19738037]
36. Gallagher D, Kelley DE, Yim JE, et al. Adipose tissue distribution is different in type 2 diabetes. Am J Clin Nutr. 2009; 89:807–814. [PubMed: 19158213]
37. Durheim MT, Slentz CA, Bateman LA, Mabe SK, Kraus WE. Relationships between exercise-induced reductions in thigh intermuscular adipose tissue, changes in lipoprotein particle size, and visceral adiposity. Am J Physiol Endocrinol Metab. 2008; 295:E407–E412. [PubMed: 18544640]

Key Points

- Fat infiltration of muscle commonly occurs in many metabolic and neuromuscular diseases.
- Image-based semi-quantitative classifications for assessing fat infiltration are not well validated.
- Quantitative MRI techniques provide an accurate assessment of muscle fat.

Fig 1.
T2-weighted image of the calf illustrating the manual segmentation of the six muscle compartments of the calf. *AC* anterior compartment, *SOL* soleus, *DP* deep posterior compartment, *MG* medial gastrocnemius, *LG* lateral gastrocnemius and *LC* lateral compartment

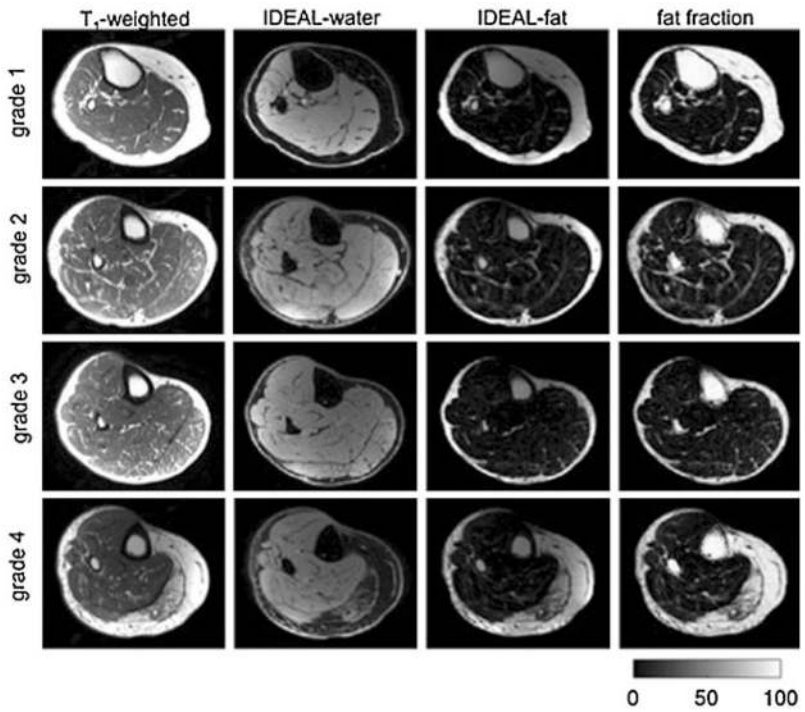

Fig 2.

Representative water/fat separation MR images for the Goutallier classification 0–4 in the medial gastrocnemius muscle: T1-weighted image, water separated image, fat-separated image and fat fraction map. *Grey scale* corresponds to fat fraction values as percentages

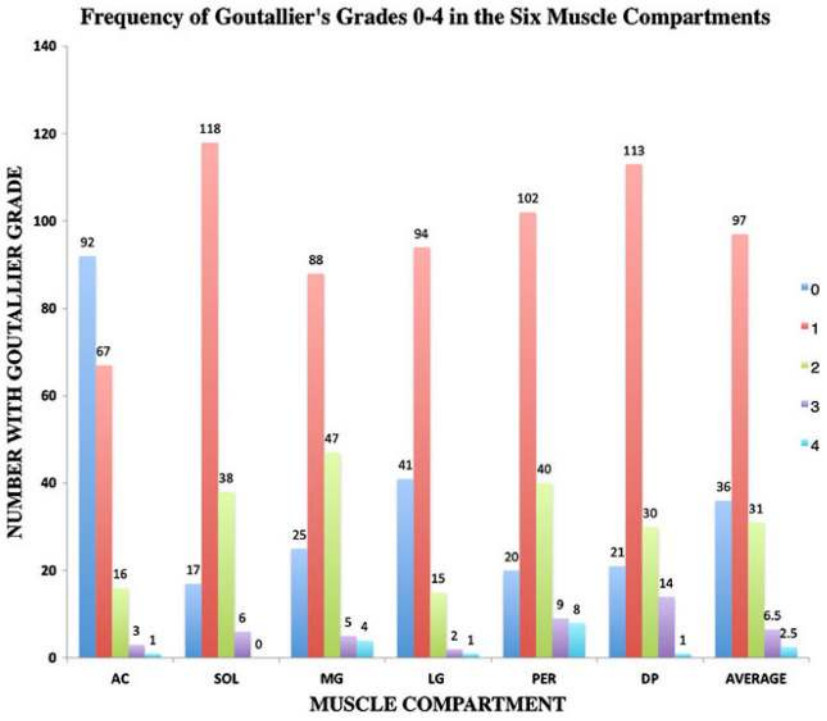

Fig 3.

Frequency of different Goutallier grades in the six muscle compartments in the whole calf averaged and in the individual compartments

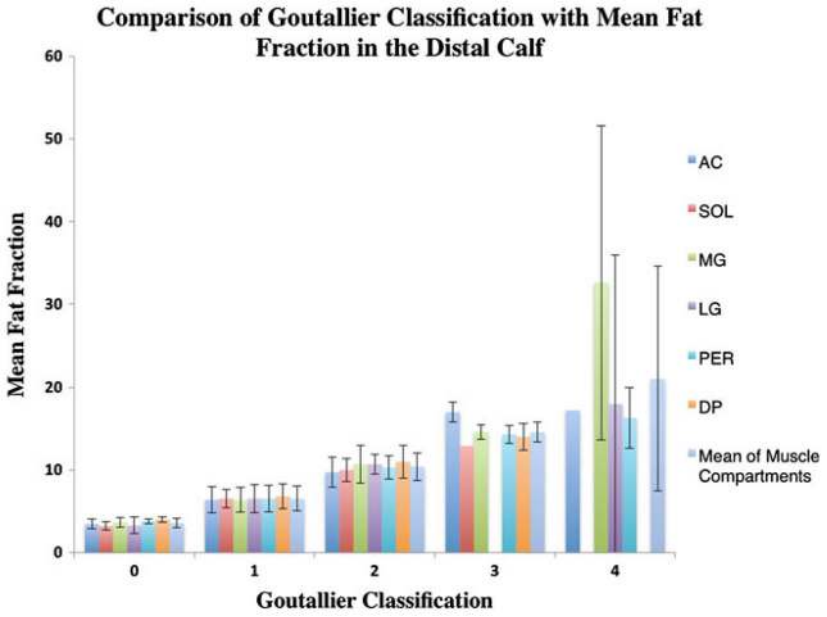

Fig 4.

Mean fat fraction in the distal calf according to the Goutallier classification averaged for all compartments and for the individual compartments

Table 1

Mean and standard deviation of IDEAL-derived fat fraction values for each Goutallier grade in the proximal calf, averaged for the individual compartments and all compartments. The mean fat fraction is significantly different among clinical grades for all muscle compartments (all $P<0.0001$)

Fat fraction percentage by muscle compartment							
Goutallier grade	**AC Mean ± SD**	**SOL Mean ± SD**	**MG Mean ± SD**	**LG Mean ± SD**	**LC Mean ± SD**	**DP Mean ± SD**	**Average of compartments Mean ± SD**
0	3.04±0.8 *n*=33	3.84±0.6 *n*=7	3.48±0.8 *n*=5	3.47±0.6 *n*=11	3.75±0.4 *n*=7	3.47±1.0 *n*=10	3.51±0.7
1	6.18±1.3 *n*=17	6.57±1.3 *n*=37	6.46±1.3 *n*=38	6.23±1.2 *n*=37	6.50±1.3 *n*=32	7.31±2.5 *n*=28	6.54±1.5
2	8.31±1.7 *n*=4	10.5±1.1 *n*=8	9.31±1.4 *n*=10	9.23±1.0 *n*=5	9.82±0.9 *n*=11	11.0±0.9 *n*=11	9.70±1.2
3	14.0 *n*=1	13.3±1.0 *n*=3	13.8±1.3 *n*=2	13.8 *n*=1	13.2±4.2 *n*=2	15.6±3.0 *n*=6	14.0±2.4
4					20.0±3.3 *n*=3		20.0±3.3

AC anterior compartment, *SOL* soleus, *MG* medial gastrocnemius, *LG* lateral gastrocnemius, *LC* lateral compartment, *DP* deep posterior compartment

Eur Radiol. Author manuscript; available in PMC 2013 July 01.

Table 2

Mean and standard deviation of IDEAL-derived fat fraction values for each Goutallier grade in the middle calf, averaged for the individual compartments and all compartments. The mean fat fraction is significantly different among clinical grades for all muscle compartments (all $P<0.0001$)

Fat fraction percentage by muscle compartment							
Goutallier grade	**AC Mean ± SD**	**SOL Mean ± SD**	**MG Mean ± SD**	**LG Mean ± SD**	**LC Mean ± SD**	**DP Mean ± SD**	**Average of compartments Mean ± SD**
0	2.93±0.8 *n*=38	3.46±0.6 *n*=6	3.18±0.9 *n*=6	3.77±0.6 *n*=15	3.99±0.5 *n*=7	3.93±0.3 *n*=6	3.54±0.6
1	6.16±1.3 *n*=20	6.79±1.3 *n*=43	6.02±1.2 *n*=33	6.02±1.1 *n*=37	6.50±1.1 *n*=36	6.71±1.3 *n*=42	6.4±1.2
2	8.02±4.7 *n*=4	9.47±2.3 *n*=11	9.72±1.3 *n*=21	8.39±2.2 *n*=6	9.93±1.0 *n*=13	10.3±1.8 *n*=8	9.3±2.2
3		11.7±1.2 *n*=2	21.3 *n*=1	12.93 *n*=1	13.9±1.4 *n*=4	13.4±1.1 *n*=5	14.6±1
4			17.07 *n*=1		17.26±0.4 *n*=2	16.7 *n*=1	17.0±0.4

AC anterior compartment, *SOL* soleus, *MG* medial gastrocnemius, *LG* lateral gastrocnemius, *LC* lateral compartment, *DP* deep posterior compartment

Table 3

Mean and standard deviation of IDEAL-derived fat fraction values for each Goutallier grade in the distal calf, averaged for the individual compartments and all compartments. The mean fat fraction is significantly different among clinical grades for all muscle compartments (all $P<0.0001$)

Fat fraction percentage by muscle compartment							
Goutallier grade	**AC Mean ± SD**	**SOL Mean ± SD**	**MG Mean ± SD**	**LG Mean ± SD**	**LC Mean ± SD**	**DP Mean ± SD**	**Average of compartments Mean ± SD**
0	3.47±0.6 *n*=21	3.22±0.5 *n*=4	3.66±0.6 *n*=14	3.29±1.0 *n*=15	3.80±0.3 *n*=6	3.98±0.3 *n*=5	3.57±0.5
1	6.40±1.6 *n*=30	6.53±1.1 *n*=38	6.36±1.5 *n*=17	6.53±1.7 *n*=20	6.53±1.6 *n*=34	6.80±1.5 *n*=43	6.53±1.5
2	9.72±1.8 *n*=8	10.0±1.4 *n*=19	10.7±2.3 *n*=16	10.7±1.2 *n*=4	10.3±1.4 *n*=16	11.0±2.0 *n*=11	10.4±1.7
3	17.0±1.2 *n*=2	12.9 *n*=1	14.6±0.9 *n*=2		14.4±1.1 *n*=3	14.0±1.6 *n*=3	14.6±1.2
4	17.2 *n*=1		32.6±19 *n*=4	17.98 *n*=1	16.3±3.7 *n*=3		21.0±11.3

Table 4

Spearman's correlations between the muscle fat fraction derived using the MRI chemical shift-based water/fat separation technique and the semi-quantitative Goutallier grade (*R*, adjusted by Bonferroni correction); all *P* values<0.0001

Muscle compartment	Proximal calf	Middle calf	Distal calf	Mean correlation
AC	0.859	0.786	0.891	0.845
DP	0.866	0.812	0.766	0.815
LG	0.810	0.798	0.894	0.834
MG	0.764	0.878	0.937	0.860
PER	0.867	0.890	0.884	0.880
SOL	0.828	0.684	0.860	0.791
Mean	0.832	0.808	0.872	

PER peroneal